

Research Article

Predicting the Effects of Coevolution on Rubisco: A Study on Carbon Dioxide Fixation by Bryophytes

Khushbu Anand¹, Afroz Alam¹

1. Department of Bioscience and Biotechnology, Banasthali University, India

Bryophytes, among the first branching terrestrial plants, has the ability to alleviate the greenhouse effect by lowering atmospheric CO₂ concentrations. In bryophytes, carbon fixation is facilitated by the enzyme Rubisco within the photosynthetic Calvin–Benson–Bassham cycle. Under conditions of low CO₂ concentration relative to O₂, the regulation of Rubisco activity can be achieved by incorporating alternative substrates that resemble RuBP, such as 2-CABP, to mitigate unproductive oxygenation reactions and enhance both photosynthetic rates and carbon fixation. This work examines the Rubisco sequences in three bryophyte taxa: liverworts, hornworts, and mosses, to identify coevolving groups implicated in the process of resistance to 2-CABP, which eventually influences carbon fixation by activating photorespiration. ClustalOmega was employed to produce a MSA methodology of filtered protein sequences utilising default settings. Furthermore, PhyML generated the phylogenetic tree using the obtained alignment. CoMap v1.5.2, utilising a compensation and grouping methodology, was utilised to identify coevolving residues. The whole structure of Rubisco proteins was not located in the PDB. The AlphaFold Protein Structure Database supplied the structure of the Rubisco protein. Furthermore, four distinct tools—I-TASSER, PyMOL V2.2.3, PSIPRED, and DSSP—forecasted the secondary structural state of residues. The pooled forecasts of a minimum of three instruments were considered. Coevolving residues are in binding, active, and secondary structures. With the DynaMut online service, point mutations' effects on protein dynamics and stability were examined in the Rubisco structure. One coevolving amino acid was a point mutation. The 2-CABP-Rubisco complex can significantly contribute to the reduction of greenhouse gases in the environment. Aspartic acid (acidic), Asparagine (non-charged polar), Histidine, and Tyrosine coevolve in bryophytes. Mutant hornworts have considerably fewer conserved residues than wild kinds, suggesting that mutation disrupts target protein function.

Introduction

In the era of global warming, an enormous increase in greenhouse gases (GHGs) by every passing day. The ecology faces significant threats from climate change. The primary objective currently must be to diminish greenhouse gases, including carbon dioxide, methane, water vapour, and nitrous oxide^[1]. Bryophytes, among the first evolving terrestrial plants, has the ability to alleviate the greenhouse effect by lowering atmospheric CO₂ concentrations^[2]. On the other hand, they would play crucial ecological roles by efficiently capturing and utilizing light energy, promoting their growth and biomass production which in turn contributes to ecosystem productivity, nutrient cycling, soil stabilization, and habitat creation for other organisms in various terrestrial ecosystems, including forests, wetlands, and tundra.

Rubisco (ribulose-1,5-bisphosphate carboxylase/oxygenase) is an enzyme that catalyses the photosynthetic Calvin-Benson-Bassham cycle in bryophytes, facilitating carbon fixation. Rubisco facilitates two separate reactions: the carboxylation of ribulose-1,5-bisphosphate (RuBP) yielding two molecules of 3-phosphoglycerate (3-PGA) and the oxygenation of RuBP resulting in phosphoglycolate and 3-PGA during photorespiration^[3]. Glycolate can impede photosynthesis and development if not adequately metabolised or recycled via the photorespiratory route, which requires energy and releases fixed CO₂^[4]. Glycolate can impede photosynthesis and development if not adequately metabolised or recycled via the photorespiratory route, which requires energy and releases fixed CO₂^[4]. Thus, Rubisco plays a major role in determining the efficiency of CO₂ assimilation and ultimately influences the photosynthetic rate.

In the condition of low CO₂ concentration as compared to O₂, the regulation of Rubisco activity can be done by involving other substrate resembling RuBP, i.e. 2-CABP (2-carboxy-d- arabinitol-1,5-bisphosphate) to avoid wasteful oxygenation reactions and improve photosynthetic rates as well as the carbon fixation. Unfortunately, the tolerance to 2-CABP is reported in some species which creates an alarming situation to study the mechanism which is making Rubisco fit against 2-CABP to maintain its nature^[5]. One of the well-known processes is alteration in the structure which is accompanied by a pattern of other alteration in protein known as coevolution to maintain the structure as well as function of protein.

In this study we study the sequences of Rubisco in three different bryophytes including liverworts, hornworts and mosses to find the coevolving groups involved in mechanism of tolerance against 2-CABP ultimately affecting carbon fixation by activating photorespiration^{[6][7][8][9]}. Further, we analyze the structure of Rubisco, which exhibits highly complex quaternary structures consisting of large subunits (L) having an active site for catalysis and small subunits (S) for maintaining enzyme's stability and assembly, to check stability of protein and identify coevolving groups affecting the tolerance at most.

Methodology

Protein Sequence Selection

A comprehensive literature review was conducted to investigate the interaction between Rubisco bound to 2-CABP and its influence on carbon fixation in bryophytes. Protein sequences from liverworts, hornworts, and mosses were retrieved from the UniProt database ([UniProt](#); IDs: B0YPN8, Q67FV0, and Q31795). The structural and evolutionary effects of 2-CABP on Rubisco, especially its binding adaptation, were examined using data from PubChem ([PubChem](#)). To enrich the dataset with homologous sequences, BLAST was utilized. Sequences that were incomplete, ambiguous, uncharacterized, or not derived from the targeted bryophyte groups were excluded from further analysis.

Phylogenetic Tree Reconstruction through MSA

Filtered protein sequences were aligned using ClustalOmega^[10] with default parameters. A phylogenetic tree was subsequently generated using PhyML^[11], applying the LG substitution matrix^[12] for improved modeling of amino acid replacements. The resulting alignment and tree were foundational for downstream coevolutionary analysis.

Detection of Coevolving Residues

Coevolving amino acid positions were identified with CoMap v1.5.2^{[13][14]}, which detects co-substituted residues that evolve in tandem along shared branches of the phylogenetic tree. This analysis incorporated multiple factors, including aligned sequences, the phylogenetic tree, a chosen substitution model, and site-specific rate variation.

Physicochemical properties like charge, polarity, volume, and Grantham scores were applied as weights for amino acid replacements. To determine statistical significance ($p \leq 0.05$) and control the false discovery rate, 1,000 bootstrap parametric runs were performed in R. Visual representation of coevolving residues was generated as a circular plot using Circos^[15].

Each residue in the multiple sequence alignment (MSA) was classified with a masking scheme (Table 1; Vats & Shanker^[16]; Hecht, Tran, & Fogel^[17]) to assign the amino acid to a specific class, facilitating a deeper understanding of coevolutionary patterns.

Class of Residue	Mask	Amino Acids
Acidic	A	Aspartic acid, Glutamic acid
Basic	B	Arginine, Lysine
Hydrophobic (non-aromatic)	H	Alanine, Leucine, Isoleucine, Valine, Methionine
Polar (non-charged)	P	Serine, Threonine, Cysteine, Asparagine, Glutamine
Aromatic	R	Phenylalanine, Tyrosine, Tryptophan, Histidine
Proline	Pr	Proline
Glycine	G	Glycine

Table 1. Amino acid residue mask based on residue class.

Analyzing the Secondary Structure of Coevolving Residues

Since the complete structure of the Rubisco protein was not available in the Protein Data Bank (PDB), it was retrieved from the AlphaFold databank^{[18][19]}. The secondary structure of the residues was predicted using four distinct tools: I-TASSER^[20], PyMOL V2.2.3^[21], PSIPRED^[22], and DSSP^[23]. A consensus approach was adopted, where predictions from at least three tools were considered. The coevolving residues identified were subsequently mapped onto binding sites, active sites, and elements of the secondary structure.

Assessing the Impact of Coevolving Residues on Structural Stability

Coevolving residue groups located in the secondary structure, binding sites, and active sites were used as mutation targets in the native Rubisco structure. Structural stability was evaluated using the DynaMut web server^[24], which analyzes how point mutations affect the protein's dynamics and stability. One coevolving amino acid was initially selected for point mutation, and the effect of subsequent mutations within the same coevolving group was assessed through the mutant PDB structure.

Molecular Docking Analysis

The AlphaFold-predicted structures of Rubisco (B0YPN8, Q67FV0, and Q31795) were used as receptors. Molecular docking simulations were conducted with AutoDock Vina v1.1.2^[25] using the ligand 2-CABP, which was obtained from the PubChem database (<https://pubchem.ncbi.nlm.nih.gov>). Kollman united atom charges were assigned to the receptor protein and ligands within the PDBQT file^[26]. Rigid docking was performed to

explore all potential binding orientations. The binding pocket residues were fixed, with a grid point spacing of 0.375 Å, and the ligand's rotatable bonds were kept flexible. A grid box with 46 points was created, centered around the binding site, to encompass all possible binding conformations.

Results

Identification of Coevolving Groups in Rubisco

To detect coevolving protein groups, 417 homologous sequences were analyzed. Across group sizes ranging from 2 to 10, a total of 35 coevolving clusters were identified, considering different biochemical properties: charge (4 groups), Grantham distance (10 groups), polarity (13 groups), and volume (9 groups) (Fig. 1). Out of Rubisco's 475 amino acids, 72 residues (15.16%) exhibited coevolution. Among these, 35 residues were part of secondary structures, including 39 helices and 5 beta sheets, accounting for 48.61% of the coevolving residues. These findings are consistent with prior studies, which suggest that coevolution often affects regions critical to structural stability^{[27][28]}. Notably, residue position 294, part of coevolving group 17 (Table 2), was identified as a binding site, warranting further investigation.

MSA used for the analysis is provided in Supplementary File 1 (SF1). Supplementary File 2 (SF2) lists the identified coevolving groups, while Supplementary File 3 (SF3) classifies the amino acid residues into classes. Supplementary File 4 (SF4) details the relative positions of the residues post-alignment and their absolute positions before MSA. The distinction between SF2 and SF3 lies in the classification of residue types, which helps understand how mutations leading to similar biochemical properties influence conservation. This classification also sheds light on the metabolic roles and distribution patterns of amino acids involved in coevolution.

The majority of coevolving residues were hydrophobic, non-aromatic amino acids (residue mask N: A, I, L, M, V), representing 40.12% of positions. These residues are considered crucial elements in maintaining structural stability. Polar, uncharged residues (Q: C, N, Q, S, T) made up 16.83%, while basic residues (B: K, R) accounted for 15.43%. Acidic residues (A: D, E) contributed 10.25%, aromatic residues (R: F, H, W, Y) made up 10.13%, proline accounted for 5.67%, and glycine was the least represented at 1.57%.

S.No. In SF2#	Coevolving groups	Size	p-value	weight ^Λ	FDR*
34	D/N293; H/Y301 A/Q286; R294 Site 293(286) ¶ ;Helix; amino acid D Site 301(294) ¶ ;Sheet; amino acid H	2	0.002	Charge	yes

Table 2. The coevolving group, along with their corresponding amino acid residue classes (in bold) and associated secondary structures.

#: Serial number of coevolving groups (refer to SF2)

¶: Site — Relative position after MSA (absolute position before MSA)

^Λ: Biochemical property considered for coevolution analysis

*: FDR — False Discovery Rate

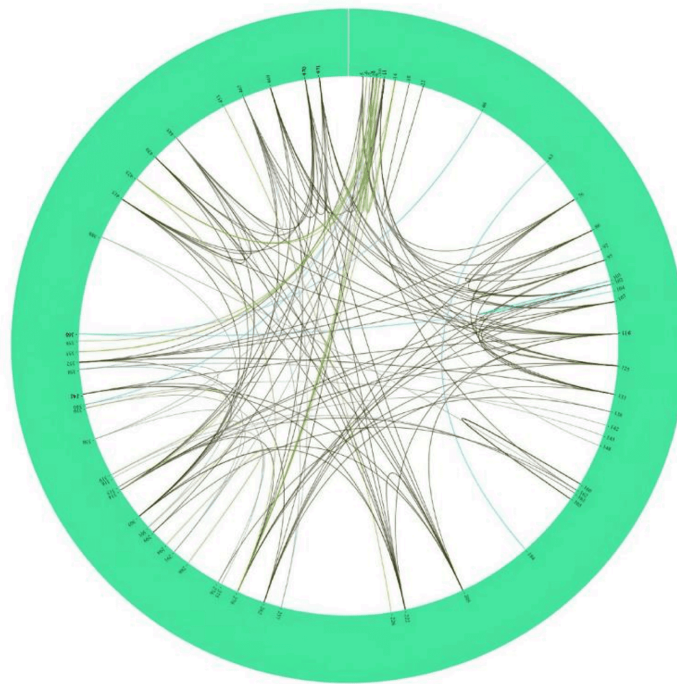


Figure 1. The circular plot illustrates the coevolving amino acid groups identified in Rubisco. The outer green circle displays the relative positions of amino acids within the multiple sequence alignment that are part of coevolving groups. Colored links represent coevolving interactions, categorized by weighted substitutions: Grantham (dark green), polarity (green), volume (blue), and charge (sky blue).

Bryophyte Class	Mutation	DynaMut	mCSM	SDM	DUET
Liverwort	D286N	-0.73	-0.364	-0.39	0.2
	D286N + H294Y	0.8	0.52	-1	0.39
Hornwort	D286N + H294Y	0.98	0.53	-0.84	0.44
Mosses	D286N + H294Y	0.9	0.6	-0.25	0.54

Table 3. Change in the stability of Rubisco induced by mutation of coevolving residues.

Secondary Structure Analysis

Mapping the coevolving sites in Rubisco reveals that residues within helices are more likely to coevolve (85.71%) compared to those in beta sheets (14.29%), as shown in Supplementary Table 1 (ST1). To understand the influence of coevolution on Rubisco's structural stability and function, we focused on coevolving group 34 (SF2) within the L-subunit, analyzing its amino acid composition and inter-residue distance to pinpoint coevolution sites.

Research has demonstrated that residues at homo-oligomeric interfaces can coevolve even when separated by more than 15 Å in protein structures^{[16][29]}. This suggests that spatially distant residues may still experience evolutionary pressures. Considering the importance of Rubisco in carbon fixation — and its link to global climate processes — mutations at coevolving positions could impact this essential function. To explore this, we investigated structural changes resulting from two mutations (D286N and H294Y) in coevolving group 9 (Table 3). Each mutation was analyzed individually to evaluate its impact on Rubisco's 3D structure. Stability analysis through the DynaMut2 server (Table 3) indicated that these mutations may enhance the structural stability of Rubisco.

It has been suggested that even without direct physical interactions, mutations can trigger significant evolutionary shifts in amino acid composition. Our findings support the idea that nature-driven coevolution in Rubisco might have evolved as a protective mechanism to maintain function despite evolutionary pressures, potentially enhancing resistance to inhibitors like 2-CABP.

Coevolution-Induced Changes in Rubisco L-Domain Interaction Patterns

To investigate how coevolution influences the binding affinity of Rubisco for the inhibitor 2-CABP, molecular docking was performed using active and binding site residues identified in UniProt. The L-subunit of Rubisco contains binding domains for substrates like RuBP and its analogs^[2], while the S-subunit contributes to the complex's structural assembly^[30].

For the docking analysis, the highest-ranked structure within the cluster was selected. A thorough search was conducted to determine the optimal binding pose for each docked ligand, ensuring that the atoms occupied the most energetically favorable positions within the complex. The conformation with the lowest root-mean-square deviation (RMSD) values was chosen for further analysis, providing insights into how coevolution-driven mutations might alter Rubisco's binding dynamics.

Bryophyte Class	Rubisco	Binding affinity(Kcal/mol)
Liverwort	Wild	-7.0
	Mutant	-5.6
Hornwort	Wild	-7.0
	Mutant	-6.0
Moss	Wild	-7.1
	Mutant	-6.0

Table 4. Binding Affinity Changes in Docked Structures of Wild-Type and Mutant Rubisco

Binding Affinity Analysis in Liverwort Rubisco Docking

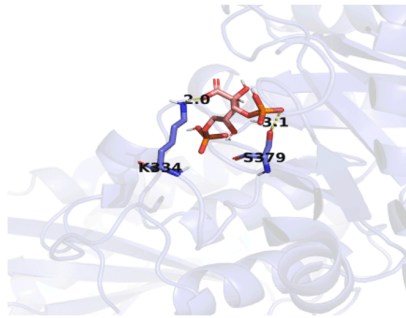
When Rubisco was docked with 2-CABP, the docked conformation showed root-mean-square deviation (RMSD) values of 0.62 Å for all ligand atoms and 0.08 Å for the C-alpha atoms (Fig. 2). In the wild-type complex, the coevolving residue H294 in the L-subunit, specifically the HE2 atom, formed interactions with the O2 and O5 atoms of the ligand. However, in the mutant complex, residue H294 is replaced by tyrosine (Y294), where the HH atom interacts with the ligand's O6 atom (Fig. 3A).

This reduced interaction in the mutant complex suggests a lower binding affinity for the inhibitor, likely due to the bulkier aromatic ring of tyrosine introducing steric hindrance. In contrast, histidine appears to stabilize the ligand through more favorable interactions. Additionally, the ligand distance increased by 0.3 Å in the mutant complex compared to the wild-type structure. In the wild-type, the HZ1 atom of Lys334 forms a contact with the ligand's O7 atom, while in the mutant complex, the O2, O9, and O4 atoms of 2-CABP interact with the NZ and HZ2 atoms of Lys334, as well as the O10 atom of the ligand.

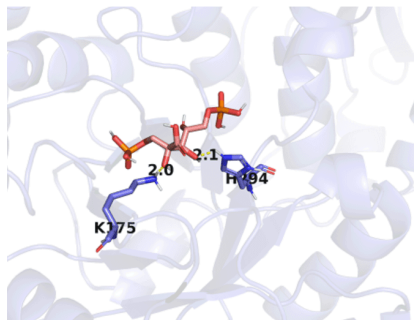
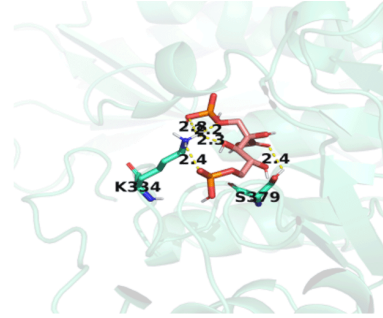


Figure 2. Docking of 2-CABP (Pink) in Liverwort Rubisco's active site in wild (Blue) and mutant (Green).

The increased interaction between lysine residues and 2-CABP may lead to steric hindrance, where the spatial arrangement of atoms in the protein's active site becomes less favorable for 2-CABP binding. The electronegative value of nitrogen (3.04) is more than Hydrogen (2.2). The bonding in mutant with nitrogen instead of hydrogen in the wild suggests significantly high biological activity and stability affecting both photosynthesis and CO₂ fixation by promoting photorespiration and preventing ligand from strong binding. The distance in mutant increased by 0.4Å from the ligand indicating less stronger bond. The binding of T173 decreased from wild to mutant such as two atoms HG1 and HN were connected to O12 of ligand while only HG1 is connected to O3 in mutant. This shows decreased binding affinity of ligand to mutant as well as change in the orientation of the 2-CABP. The distance of T173 in mutant from 2-CABP is increased by 0.7Å. The O atom of S379 was interacting with H9 of ligand in the wild but the mutant HG atom of S379 interacted with O7 of ligand showing change in conformation of inhibitor while distance increased by 0.4Å in mutant. All these increased distance from the conserved residues in native and mutant protein structure reports in the direction of increased pocket size in mutant as compared to native. In wild the two interacting glycine atom were HN of G403 and G380 both with O9 and G403 HN with O12 of ligand while G381 HN interacts with O11 and O10, G404 HN with O11 and O5 and G204 OE1 with O12, suggesting the obstruction in the binding site and making it difficult for 2-CABP to interact with its target. The connection found the same in wild and mutant is K175 HZ1 to O1 i.e. ligand changed its orientation keeping the atom O1 as axis. The other lost connection in mutant as compared to wild is H298 HE2 and R295 1HH2 and HE to O13, T173 HN to O12 and H327 HD to O3 and O11.



(A)



(B)

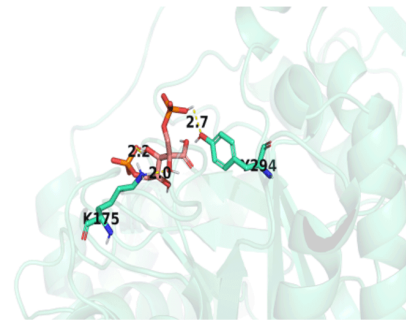


Figure 3. Liverwort's Rubisco docked structure of wild (Blue) and mutant (green) with the ligand 2-CABP (pink) A) binding site 334 & 379 B) binding site 175 & coevolution site 294

Binding Affinity Analysis in Hornwort Rubisco Docking

In the docked conformation of Rubisco with 2-CABP, the RMSD values were 1.1 Å for all ligand atoms and 0.08 Å for the C-alpha atoms. In the wild-type complex, the coevolving residue H294, located in the L-subunit sheet, forms a connection through its HE2 atom with the O2 atom of the ligand. However, this interaction is lost in the mutant complex, indicating a disruption in binding affinity. This shows a major loss in connection affecting the overall binding. The restored interaction is R295 2HH2, H298 HE2 and R295 2HH1, H298 HD1 to O11 in both wild and mutant complexes respectively while R295 HE in wild is lost abruptly losing strong interaction of target to inhibitor assisting tolerance. The increased distance shown by H298 is 0.5 Å while distance decreased in R295 by 0.3 Å which overall is increased pocket size. The lost connection are K175 HZ1 atom with O1 and O6 atom of ligand, K177 HZ2 with O6 atom, K334 HZ1 to O7, H327 HD1 to O3 and O10, T173 HG1 to O12, Q401 O to O12, G380 HN to O9 and G403 HN to O9 and O12 while new build interaction are Q336 O to H9 and H10, Q336 HN to O13, Q338 HN to O8 and O12, D473, OD2 and O to H12 and R303 1HH1 to O11 in wild and mutant respectively. This

suggests huge steric hindrance in the target which may affect the stability as well as conformation and ultimately the function

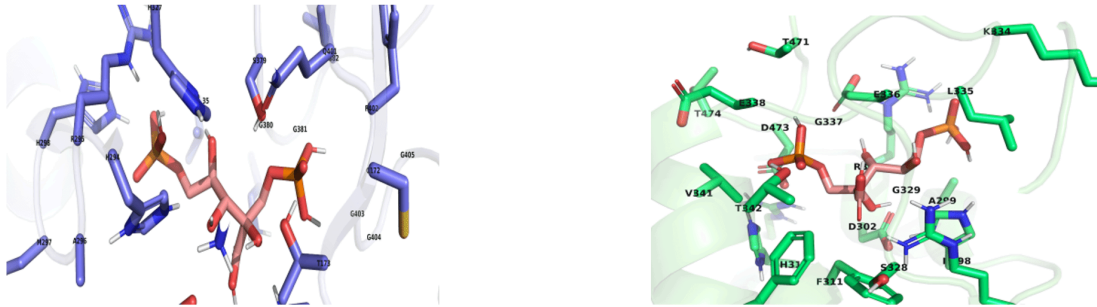
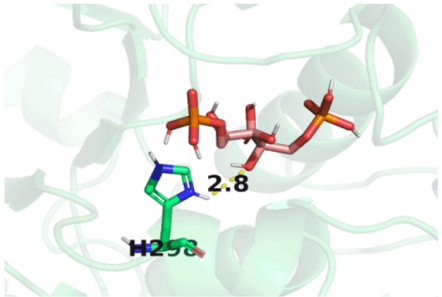
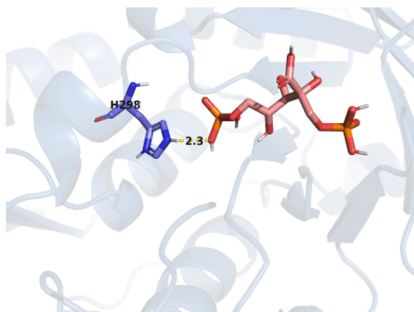
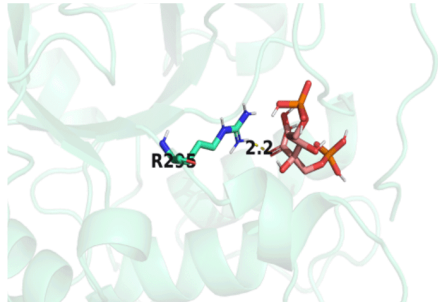
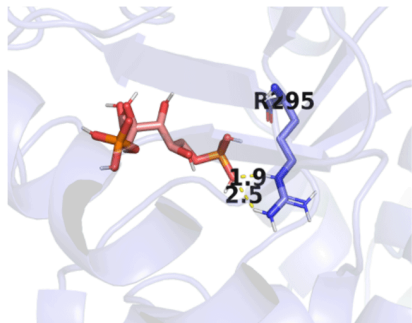


Figure 4. Docking of 2-CABP (Pink) in hornwort Rubisco's active site in wild (Blue) and mutant (Green)



(A)



(B)

Figure 5. Hornwort's Rubisco docked structure of wild (Blue) and mutant (green) with the ligand 2-CABP (pink) A) binding site 298 B) binding site 295

Mosses

The rmsd of all atoms and C-alpha atom in 2-CABP's docked conformation were 0.26 Å and 0.08 Å, respectively, when it was docked with Rubisco. The coevolving as well as binding residue H294 HE2 with O2 of ligand in wild while the connection is lost in mutant, that means binding of ligand is severely affected. The conserved bonds are R295 1HH2, HE to O11, H298 HE2 to O11, H327 HD1 to O10 and K177 HZ2 to O7 in both wild and mutant while their distances increased by 0.2, 0.2, 0.1 and 0.4 Å respectively by residues with no change distance of R295 1HH2. The little change in atoms connected overall bond was conserved is seen in H327 HD1 to O10 and O3, G403 HN to O8, O9 and O8, O12, S379 O to H13 and HG to O1, K175 HZ1 to O12 and O4, O6, G404 HN to O12 and O8 in wild and mutant respectively. The distances varies in mutant by .The lost connections in the wild are G4380 HN to H11 and T173 to O1. The new build interactions in mutant are K334 HZ1 to O2, HZ2 to O9, and G204 OE2 to H10. The residues interacting with ligand are more in mutant but the binding energy is seen to be increased which signifies that target-ligand complex is less stable may be due to steric hindrances, unfavourable changes in conformation affecting dynamics and function.

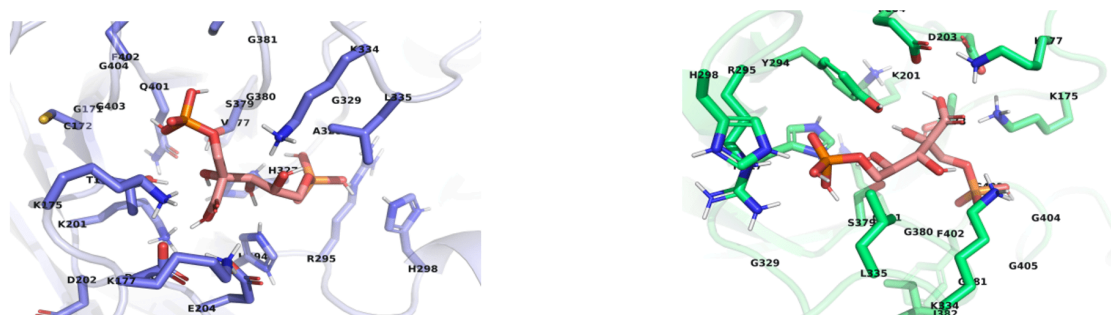


Figure 6. Docking of 2-CABP (Pink) in mosses Rubisco's active site in wild (Blue) and mutant (Green).

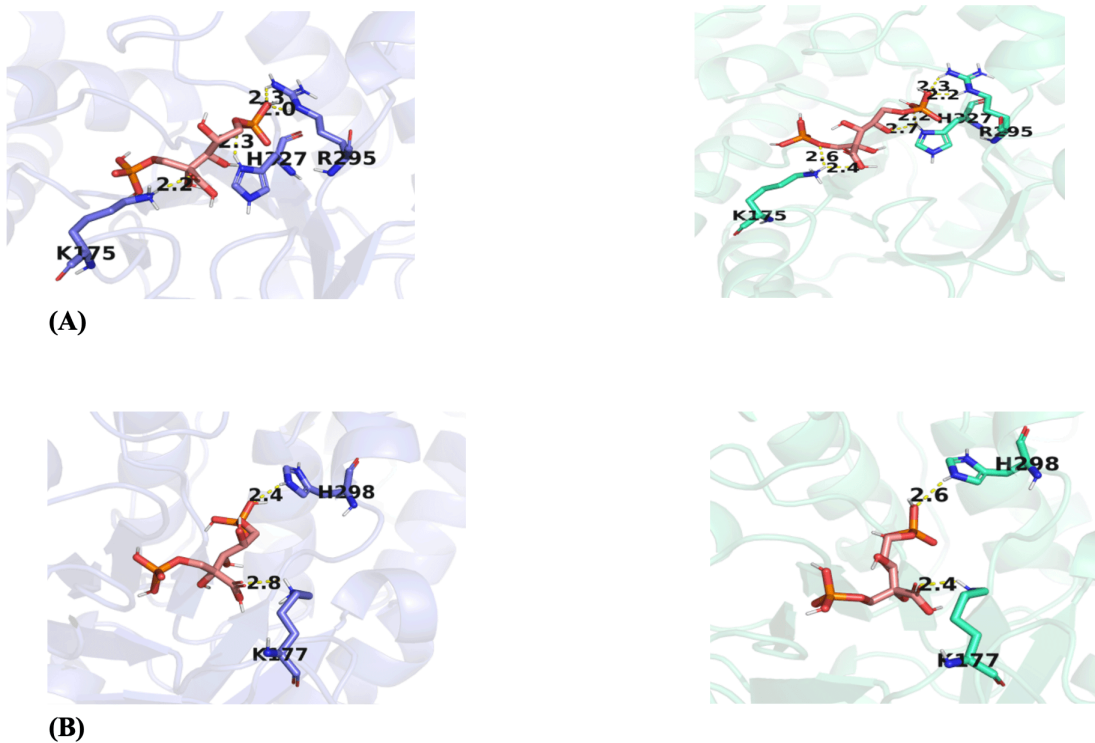


Figure 7. Hydrogen Bond Interactions in Mosses Rubisco Docked Structures. The hydrogen bond interactions in mosses Rubisco are shown for both wild-type (blue) and mutant (green) structures docked with the ligand 2-CABP (pink). Interactions are observed at the following binding sites: (A) Sites 175, 327, and 295 (B) Sites 177 and 298.

Discussion

This study highlights a coevolution-driven mechanism that alters the conformation of Rubisco's active site, contributing to inhibitor tolerance. We examined the structural stability of the Rubisco protein complexed with 2-CABP, an inhibitor that plays a crucial role in reducing photorespiration. Targeting Rubisco through inhibitor therapy remains a promising strategy for enhancing CO₂ fixation and improving photosynthesis efficiency. The interaction between 2-CABP and Rubisco could have significant environmental benefits by lowering greenhouse gas (GHG) emissions. Understanding the structural alterations driven by coevolution can inform the development of improved inhibitors that adapt to future evolutionary changes in Rubisco. In bryophytes, key coevolving residues include aspartic acid (acidic), asparagine (polar, uncharged), histidine, and tyrosine (aromatic), all of which may influence Rubisco's response to inhibitors and overall enzymatic function. The mosses are reported to contribute most in CO₂ fixation as compared to other bryophytes due to its abundance. In this study we can support this by interpreting the more residues are conserved between wild and mutant which means binding could be less affected leading to positive indicators for enhanced photosynthesis

resulting in more CO₂ fixation as well as increased production of biomass. The additional benefit of moss species is water retention to a huge extent which in turns maintains hydrological cycles. The hornworts are found to have much less conserved residues in mutant compared to wild which more probably means a disruption in function of target protein due to impact of mutation. A well-known fact is there are less species of hornwort reported till date and mutation can badly affect the existence of hornwort pointing towards an alert of nature to the humans. The other known significance of hornwort is nutrient cycling and soil formation by colonizing barren moist land to help different plant species establish themselves. Our work suggests that if ligand is enhanced according to coevolving residues, then the function of protein can be revived expecting a better outcome for the earth as well as organisms surviving on it. The liverwort is also in a good state as it conserves the binding as well as coevolving residue which shows that the adverse effect of coevolution is somehow fixed and performance can be restored to extent defining a stable condition till few coming years. The liverwort has been associated with indicators of environmental health, so this study can somehow establish that its state manifests the survival of organisms on the earth after all these drastic climatic changes. The one most important point to be discussed is that all three bryophyte classes are sensitive to rise in temperature but they are surviving, the research focuses on the places where they exist and a little effort towards them would bring back a lot to our earth.

Conclusion

Our study shows the significance of Bryophytes to the whole ecosystem and its threats and ways to enhance their function and let them contribute more to the environment. The balancing of GHGs can prevent a lot of emerging issues and diseases. Once the ligand 2-CABP modified according to coevolving groups and used in the areas where bryophytes are abundant, expected results could be seen. The coevolving groups found could be considered to prevent a tolerance of protein to inhibitor. This also gives us a lead that ligands other than 2-CABP could be used or other methods could be discovered to use bryophytes for reducing CO₂ by increasing its fixation which in turn would enhance photosynthesis as well as biomass production.

References

1. [△]Rogelj J, Shindell D, Jiang K, Fifita S, Forster P, Ginzburg V, Handa C, Kheshgi H, Kobayashi S, Krieglner E, Mundaca L (2018). *Mitigation pathways compatible with 1.5 C in the context of sustainable development. In Global warming of 1.5 C (pp. 93-174). Intergovernmental Panel on Climate Change.*
2. [△][△]Andersson I, Backlund A (2008). "Structure and function of Rubisco". *Plant Physiology and Biochemistry.* 46(3): 275-91.

3. [^]Caemmere SV (2020). Rubisco carboxylase/oxygenase: from the enzyme to the globe: A gas exchange perspective. *Journal of Plant Physiology, ScienceDirect* 153240(252):1-12. Hanson DT, Rice SK (2013). What can we learn from Bryophyte Photosynthesis. *Photosynthesis in Bryophytes and Early Land Plants Advances in Photosynthesis and Respiration* 37: 1-8.
4. [^][^]Fernie AR, Bauwe H (2020). "Wasteful, essential, evolutionary stepping stone? The multiple personalities of the photorespiratory pathway". *The Plant Journal*. 102(4):666-77.
5. [^]Tommasi IC (2021). "The mechanism of Rubisco catalyzed carboxylation reaction: chemical aspects involving acid-base chemistry and functioning of the molecular machine". *Catalysts*. 11(7):813.
6. [^]Rai GP, Shanker A (2024). "Coevolution-based computational approach to detect resistance mechanism of epidermal growth factor receptor". *Biochimica et Biophysica Acta (BBA)-Molecular Cell Research*. 1871(1):119592.
7. [^]Priya P, Shanker A (2021). "Coevolutionary forces shaping the fitness of SARS-CoV-2 spike glycoprotein against human receptor ACE2". *Infection, Genetics and Evolution*. 87:104646.
8. [^]Sandler I, Zigdon N, Levy E, Aharoni A (2014). "The functional importance of co-evolving residues in proteins". *Cellular and Molecular Life Sciences*. 71:673-82.
9. [^]S. Chakrabarti, A.R. Panchenko (2010). Structural and functional roles of coevolved sites in proteins, *PLoS One* 5 (1) e8591.
10. [^]Sievers F, Higgins DG (2014). "Clustal Omega, accurate alignment of very large numbers of sequences". *Multiple Sequence Alignment Methods*. 105-16.
11. [^]Guindon S, Dufayard JF, Hordijk W, Lefort V, Gascuel O (2009). "PhyML: fast and accurate phylogeny reconstruction by maximum likelihood". *Infection Genetics and Evolution*. 9:384-385.
12. [^]Le SQ, Gascuel O (2008). "An improved general amino acid replacement matrix". *Molecular Biology and Evolution*. 25(7):1307-20.
13. [^]Dutheil J, Pupko T, Jean-Marie A, Galtier N (2005). "A model-based approach for detecting coevolving positions in a molecule". *Molecular Biology and Evolution*. 22(9):1919-28.
14. [^]Dutheil J, Galtier N (2007). "Detecting groups of coevolving positions in a molecule: a clustering approach". *BMC Evolutionary Biology*. 7:1-8.
15. [^]Yu Y, Ouyang Y, Yao W (2018). "Circos: an R/Shiny application for interactive creation of Circos plot". *Bioinformatics*. 34(7):1229-31.
16. [^][^]S. Vats, A. Shanker (2019). Groups of coevolving positions provide drug resistance to *Mycobacterium tuberculosis*: a study using targets of first-line antituberculosis drugs, *Int. J. Antimicrob Agents* 53 (3) 197-202.
17. [^]Hecht D, Tran J, Fogel GB (2011). "Structural-based analysis of dihydrofolate reductase evolution". *Molecular Phylogenetics and Evolution*. 61(1):212-30.

18. [△]J. Jumper, R. Evans, A. Pritzel, T. Green, M. Figurnov, O. Ronneberger, D. Hassabis (2021). Highly accurate protein structure prediction with AlphaFold, *Nature* 596 (7873) 583–589.
19. [△]M. Varadi, S. Anyango, M. Deshpande, S. Nair, C. Natassia, G. Yordanova, S. Velankar (2022) AlphaFold protein structure database: massively expanding the structural coverage of protein–sequence space with high-accuracy models, *Nucleic Acids Res.* 50 (D1) D439–D444.
20. [△]Zhou X, Zheng W, Li Y, Pearce R, Zhang C, Bell EW, Zhang G, Zhang Y (2022). "I-TASSER-MTD: a deep-learning-based platform for multi-domain protein structure and function prediction". *Nature Protocols.* 17(10):2326–53.
21. [△]L.L.C. Schrödinger, W. Delano (2020). *The PyMOL Molecular Graphics System, Version 2.2.* 3.
22. [△]L.J. McGuffin, K. Bryson, D.T. Jones (2000). "The PSIPRED protein structure prediction server". *Bioinformatics.* 16 (4):404–405.
23. [△]Zacharias J, Knapp EW (2014). "Protein secondary structure classification revisited: processing DSSP information with PSSC". *Journal of Chemical Information and Modeling.* 54(7):2166–79.
24. [△]Rodrigues, D.E. Pires, D.B. Ascher (2018). DynaMut: predicting the impact of mutations on protein conformation, flexibility and stability, *Nucleic Acids Res.* 46: 350–355.
25. [△]O. Trott, A.J. Olson (2010). AutoDock Vina: improving the speed and accuracy of docking with a new scoring function, efficient optimization, and multithreading, *J.Comput.Chem.* 31(2):455–461.
26. [△]G.M. Morris, R. Huey, W. Lindstrom, M.F. Sanner, R.K. Belew, D.S. Goodsell, A. J. Olson (2009). AutoDock4 and Auto DockTools4: automated docking with selective receptor flexibility, *J. Comput. Chem.* 30 (16): 2785–2791.
27. [△]M.W. Dimmic, M.J. Hubisz, C.D. Bustamante, R. Nielsen (2005). Detecting coevolving amino acid sites using Bayesian mutational mapping, *Bioinformatics* 21 (suppl_1) i126–i135.
28. [△]Wang M, Kapralov MV, Anisimova M (2011). "Coevolution of amino acid residues in the key photosynthetic enzyme Rubisco". *BMC Evolutionary Biology.* 11 (1): 1–12.
29. [△]I. Anishchenko, S. Ovchinnikov, H. Kamisetty, D. Baker (2017). Origins of coevolution between residues distant in protein 3D structures, *Proc. Natl. Acad. Sci.* 114 (34): 9122–9127.
30. [△]Valegård K, Hasse D, Andersson I, Gunn LH (2018). "Structure of Rubisco from *Arabidopsis thaliana* in complex with 2-carboxyarabinitol-1, 5-bisphosphate". *Acta Crystallographica Section D: Structural Biology.* 74(1):1–9.

Declarations

Funding: No specific funding was received for this work.

Potential competing interests: No potential competing interests to declare.